Title: Microscopic and metatranscriptomic analyses revealed unique cross-domain symbiosis between *Candidatus* Patescibacteria/candidate phyla radiation (CPR) and methanogenic archaea in anaerobic ecosystems

Kyohei Kuroda[1*¶], Meri Nakajima[1,2¶], Ryosuke Nakai[1], Yuga Hirakata[3], Shuka Kagemasa[1,4,5], Kengo Kubota[5,6], Taro Q.P. Noguchi[7], Kyosuke Yamamoto[1], Hisashi Satoh[2], Masaru K. Nobu[3,8], Takashi Narihiro[1*]

[1]Bioproduction Research Institute, National Institute of Advanced Industrial Science and Technology (AIST), 2-17-2-1 Tsukisamu□Higashi, Toyohira□ku, Sapporo, Hokkaido, 062□8517 Japan

[2]Division of Environmental Engineering, Faculty of Engineering, Hokkaido University, North-13, West-8, Hokkaido, 060-8628 Japan

[3]Bioproduction Research Institute, National Institute of Advanced Industrial Science and Technology (AIST), Central 6, Higashi 1-1-1, Tsukuba, Ibaraki 305-8566, Japan

[4]Department of Civil and Environmental Engineering, National Institute of Technology, Anan College, 265 Aoki Minobayashi, Anan, Tokushima 774-0017, Japan

[5]Department of Civil and Environmental Engineering, Graduate School of Engineering, Tohoku University, 6-6-06 Aza-Aoba, Aramaki, Aoba-ku, Sendai, Miyagi 980-8579, Japan

[6]Department of Frontier Sciences for Advanced Environment, Graduate School of Environmental Studies, Tohoku University, 6-6-06 Aza-Aoba, Aramaki, Aoba-ku, Sendai, Miyagi 980-8579, Japan

[7]Department of Chemical Science and Engineering, National Institute of Technology, Miyakonojo College, 473-1 Yoshio-cho, Miyakonojo, Miyazaki, 885-8567, Japan

[8]Institute for Extra-cutting-edge Science and Technology Avant-garde Research (X-star), Japan Agency for Marine-Earth Science and Technology (JAMSTEC), 2-15 Natsushima-cho, Yokosuka, Kanagawa 237-0061, Japan

[¶]These authors contributed equally to this work.

[*]Co-corresponding authors:

Kyohei Kuroda, Tel: +81 11 857 8402; E-mail: k.kuroda@aist.go.jp

Takashi Narihiro, Tel: +81 29 861 9443; E-mail: t.narihiro@aist.go.jp

Abstract

To verify the parasitic lifestyle of *Candidatus* Patescibacteria in the enrichment cultures derived from a methanogenic bioreactor, we applied multifaceted approaches combining cultivation, microscopy, metatranscriptomic, and protein structure prediction analyses. Cultivation experiments with the addition of exogenous methanogenic archaea with acetate, amino acids, and nucleoside monophosphates and 16S rRNA gene sequencing confirmed the increase in the relative abundance of *Ca*. Patescibacteria and methanogens. The predominant *Ca*. Patescibacteria were *Ca.* Yanofskybacteria and 32-520 lineages (to which belongs to class *Ca*. Paceibacteria) and positive linear relationships ($r^2 \geq 0.70$) between the relative abundance of *Ca*. Yanofskybacteria and *Methanothrix*, suggesting that the tendency of the growth rate is similar to that of the host. By fluorescence *in situ* hybridization (FISH) observations, the FISH signals of *Methanothrix* and *Methanospirillum* cells with *Ca*. Yanofskybacteria and with 32-520 lineages, respectively, were significantly lower than those of the methanogens without *Ca*. Patescibacteria, suggesting their parasitic interaction. The TEM and SEM observations also support parasitism in that the cell walls and plugs of these methanogens associated with submicron cells were often deformed. In particular, some *Methanothrix*-like filamentous cells were dented where the submicron cells were attached. Metatranscriptomic and protein structure prediction analyses identified highly expressed secreted genes from the genomes of *Ca*. Yanofskybacteria and 32-520, and these genes contain adhesion-related domains to the host cells. Considering the results through the combination of microscopic observations, gene expression, and computational protein modeling, we propose that the interactions between *Ca*. Yanofskybacteria and 32-520 belonging to class *Ca*. Paceibacteria and methanogenic archaea are parasitism.

58 Keywords: Candidate Phyla Radiation (CPR), *Candidatus* Patescibacteria, cross-domain
59 symbiosis, *Candidatus* Yanofskybacteria/UBA5738, 32-520/UBA5633, scanning electron
60 microscopy (SEM), transmission electron microscopy (TEM), metatranscriptomic analysis
61
62

63 **Main text**

64 Candidate phyla radiation (CPR)/*Candidatus* Patescibacteria, ultrasmall bacteria, is a
65 major lineage of the domain Bacteria that is widely distributed in various natural and
66 artificial environments (1–5). To date, several *Ca*. Patescibacteria-bacteria intradomain
67 symbioses have been observed (*e.g.*, *Ca*. Saccharimonadia with Actinobacteria (6, 7) and *Ca*.
68 Gracilibacteria with Gammaproteobacteria (8, 9). Most recently, three cases of cross-domain
69 symbioses between the class *Ca*. Paceibacteria (former Parcubacteria/OD1) of the *Ca*.
70 Patescibacteria and domain Archaea have been reported by using cultivation and microscopic
71 observations, *i.e.*, *Ca*. Yanofskybacteria/UBA5738 (10) and *Ca*. Nealsonbacteria (11) with
72 aceticlastic methanogenic archaeon *Methanothrix* and 32-520/UBA5633 with the
73 hydrogenotrophic methanogen *Methanospirillum* (12). Our previous microscopic
74 observations suggested that the interactions between *Ca*. Paceibacteria and methanogenic
75 archaea are likely to cause parasitism, based on the absence or low detectable ribosomal
76 activity (based on fluorescence *in situ* hybridization [FISH]) and deformations at the
77 attachment sites (based on transmission electron microscopy [TEM]) (10, 12). In addition,
78 several genetic features that may contribute to parasitism have been identified in the
79 metagenome-assembled genomes of *Ca*. Paceibacteria (10–12); however, the challenge is to
80 maintain enrichment cultures to ensure that those genes are expressed. In the present study, to
81 uncover the underlying mechanisms of parasitic interactions between *Ca*. Paceibacteria and
82 methanogens, we attempted to perform a multifaceted approach combining cultivation and
83 microscopy along with metatranscriptomic analyses for enrichment cultures derived from
84 anaerobic bioreactors.
85
86 To set up the experimental design for these analyses, we prepared seven parallel
87 enrichment cultures (called C-1–C-7) transferred from the culture system C-d2-d1 (10),

which contains acetate, amino acids, and nucleoside monophosphates as potential growth factors for *Ca*. Patescibacteria (see Text S1). The enrichment cultures showed the production of methane gas on Days 14 and 31. We then analyzed the microbial community structures by using 16S rRNA gene amplicon sequencing on Days 7, 14, 21, and 31. The abundances of *Ca*. Yanofskybacteria OTU0011 (PMX_810_sub as the metagenomic bin), 32-520 OTU 0014 (PMX.108), and 32-520 OTU0072 (PMX.50) (Fig. S1A and S1B) during cultivation varied from 0.15–12.5%, 0.6–2.3%, and 0.1–0.87%, respectively (Fig. S2A–S2D and Text S1).

The physiological and morphological characteristics of the symbioses were confirmed by microscopic observations based on fluorescence *in situ* hybridization (FISH), TEM, and scanning electron microscopy (SEM). On Day 31, the FISH fluorescence of *Methanothrix* filaments with more than 5 *Ca*. Yanofskybacteria cells was significantly lower than that of *Methanothrix* cells without *Ca*. Yanofskybacteria cells because of the significantly larger areas with no fluorescence (Fig. 1A, $p < 0.05$). In addition, the fluorescence fractions (clear, weak, and no fluorescence) of the *Methanothrix* filaments also showed that many of the *Ca*. Yanofskybacterial cells (35±25 cells/*Methanothrix*-filamentous) were attached to *Methanothrix* with no fluorescence on Day 31 (Fig. 1B and 1D, Figs. S3A, and S4). *Methanospirillum* cells with 32-520 cells (1.1±0.3–1.3±0.5 cells/*Methanospirillum*-cell, Fig. S3B) also had significantly lower FISH signals than *Methanospirillum* cells without 32-520 (Fig. 1C and Fig. S5, $p < 0.05$). Taken together, the interactions between methanogenic archaea and *Ca*. Paceibacteria are parasitic, strongly supporting previous predictions with statistical evidence (10, 12). The TEM observations also supported the parasitism of *Ca*. Yanofskybacteria, as the cell walls of *Methanothrix* (sheathed filamentous cells) (13) were often deformed where the submicron cells were attached. Interestingly, some *Methanothrix*-like filamentous cells with submicron *Ca*. Yanofskybacteria-like cells were dented through

TEM observation (Fig. 1E–1H). In addition, the submicron cells produced adhesive materials at the attachment sites on the *Methanothrix* cells (Fig. 2A and 2B). Therefore, it is speculated that the secreted materials are important for the attachment of *Ca*. Yanofskybacteria cells to *Methanothrix* cells. Another type of submicron cell (likely 32-520 cells) was tightly attached to the plug structures of *Methanospirillum* (rod-shaped sheath cells) (Fig. 2C and 2D) (14). The TEM observations indicated that there are extracellular substances at the attachment sites of 32-520-like submicron cells (Fig. 1I and 1J). These microscopic observations imply that the production of extracellular substances is essential for the episymbiosis of *Ca*. Paceibacteria. High-resolution imaging techniques such as cryo-electron microscopy can be an effective approach to further clarify their cellular structures and attachment sites.

To confirm their interactions based on gene expression levels, we performed metatranscriptomics for the enrichment cultures on Days 14 (triplicate) and 31 (duplicate). A total of 6.0–10.8 Gb sequences were obtained and mapped to the previously reconstructed metagenome-assembled bins of *Ca*. Yanofskybacteria/UBA5738 (PMX_810_sub) and 32-520/UBA5633 (PMX.108 and PMX.50), which belonged to MWCK01 and UBA5633 at the genus level in the GTDB database (15), respectively (Fig. S1B and Text S1) (10)(12). Previous studies have suggested that the competence protein ComEC, secretion systems, pilus, and several transporters are important for the symbiosis of ultrasmall microbes, including *Ca*. Patescibacteria, with hosts (16–19). Accordingly, these genes were highly expressed in the genome of *Ca*. Yanofskybacteria PMX_810_sub on Day 14 (Table S4), suggesting their importance in symbiotic lifestyles during the early growth stage. In addition, F-type H^+-transporting ATPase proteins were highly expressed in *Ca*. Yanofskybacteria and 32-520 PMX.50 (Tables S2 and S4), which are encoded by type IV pilus assembly proteins (Table S2). In a previous study, ATPase and type IV pili were predicted to function in

attachment and motility on larger host surfaces (19). Furthermore, some active peptidase-like proteins with signal peptides (PMX_810_sub_00385, PMX_810_sub_00508, PMX.108_00125, PMX.108_00310, PMX.108_00457, PMX.108_00476, and PMX.50_00413) (Table S2) and substrate-binding proteins of amino acid/metal transport systems were found in the three *Ca*. Patescibacteria genomes (Table S4). Although the detailed functions remain unclear, the addition of external sources of amino acids and trace elements may be key factors for the successful enrichment of *Ca*. Patescibacteria.

To estimate the function of the proteins encoded by the five most highly expressed but functionally unknown genes with signal peptides, including peptidoglycan binding domains (PGBD: PMX_810_sub_00350, PMX.50_00411, and PMX.108_00302), immunoglobulin (Ig)-like folds (PMX_810_sub_00465, PMX108_00787, and PMX.108_01191), galactose-binding domain folds (PMX.50_00003), thioredoxin-like domains (PMX.108_00787), polycystic kidney disease (PKD) domains (PMX.108_01191), and type IV secretion system pilins (PMX.108_00341, PMX.50_00571, PMX.50_00607, and PMX.50_00608), the protein structures were predicted computationally (Fig. 2F and Table S2). These domains are known to be host adhesion-related proteins, such as membrane-anchored secreted proteins that bind membrane substrates (20–22). Of these, PGBD is found at the N- or C-terminus of several enzymes involved in cell wall degradation (*e.g.*, membrane-bound lytic murein transglycosylase B and zinc-containing D-alanyl-D-alanine-cleaving carboxypeptidase) (23). Interestingly, the PGBD-containing enzymes showed relatively similar structures among the three *Ca*. Patescibacteria (Fig. 2F), suggesting that these secreted uncharacterized proteins are likely to be specific and important for *Ca*. Patescibacteria-methanogen interactions.

In summary, we found that the interactions between the class *Ca*. Paceibacteria of *Ca*. Patescibacteria and methanogenic archaea are parasitism through the combination of FISH, TEM, and SEM observations and the first successful gene expression analysis of class *Ca*. Paceibacteria. In addition, we identified highly expressed secreted proteins with PGBD that have similar structures among three *Ca*. Paceibacteria. The microscopic and metatranscriptomic observations suggested that the adhesion/degradation functions of *Ca*. Paceibacteria to host methanogen cells are uniquely developed for their parasitic lifestyle. Further elucidation of the characterizations of the cell□cell interactions in detail and the establishment of refined cocultures of *Ca*. Paceibacteria and methanogens are essential to clarify the influence of ultrasmall bacteria on anaerobic ecosystems.

Acknowledgments

This study was partly supported by the Japan Society for the Promotion of Science KAKENHI JP16H07403 and JP21H01471, a matching fund between the National Institute of Advanced Industrial Science and Technology (AIST) and Tohoku University, and research grants from the Institute for Fermentation, Osaka (G-2019-1-052 and G-2022-1-014). The authors thank Riho Tokizawa, Yuki Ebara, Tomoya Ikarashi, and Maho Takai at AIST for technical assistance.

Contributions

K. Kuroda and T.N. designed this study. K. Kuroda and M.N. performed sampling, cultivation, microscopy, and sequence analysis. K. Kuroda, M.N., R.N., Y.H., S.K., K. Kubota, T.Q.P.N., K.Y., H.S., M.K.N., and T.N. interpreted the data. K. Kuroda, M.N., and

T.N. wrote the manuscript with input from all coauthors. All authors have read and approved the manuscript submission.

Conflict of Interest

The authors declare no conflicts of interest.

References

1. Jaffe AL, Castelle CJ, Banfield JF. 2023. Habitat Transition in the Evolution of Bacteria and Archaea. Annu Rev Microbiol 77:193–212.

2. Rinke C, Schwientek P, Sczyrba A, Ivanova NN, Anderson IJ, Cheng J-F, Darling A, Malfatti S, Swan BK, Gies E a., Dodsworth J a., Hedlund BP, Tsiamis G, Sievert SM, Liu W-T, Eisen J a., Hallam SJ, Kyrpides NC, Stepanauskas R, Rubin EM, Hugenholtz P, Woyke T. 2013. Insights into the phylogeny and coding potential of microbial dark matter. Nature 499:431–437.

3. Brown CT, Hug LA, Thomas BC, Sharon I, Castelle CJ, Singh A, Wilkins MJ, Wrighton KC, Williams KH, Banfield JF. 2015. Unusual biology across a group comprising more than 15% of domain Bacteria. Nature 523:208–211.

4. Naud S, Ibrahim A, Valles C, Maatouk M, Bittar F, Tidjani Alou M, Raoult D. 2022. Candidate Phyla Radiation, an Underappreciated Division of the Human Microbiome, and Its Impact on Health and Disease. Clin Microbiol Rev 35:375–384.

5. Kuroda K, Narihiro T, Shinshima F, Yoshida M, Yamaguchi H, Kurashita H, Nakahara N, Nobu MK, Noguchi TQP, Yamauchi M, Yamada M. 2022. High-rate cotreatment of purified terephthalate and dimethyl terephthalate manufacturing wastewater by a mesophilic upflow anaerobic sludge blanket reactor and the microbial ecology relevant to aromatic compound degradation. Water Res 219:118581.

6. He X, McLean JS, Edlund A, Yooseph S, Hall AP, Liu SY, Dorrestein PC, Esquenazi E, Hunter RC, Cheng G, Nelson KE, Lux R, Shi W. 2015. Cultivation of a human-associated TM7 phylotype reveals a reduced genome and epibiotic parasitic lifestyle. Proc Natl Acad Sci U S A 112:244–249.

7. Batinovic S, Rose JJA, Ratcliffe J, Seviour RJ, Petrovski S. 2021. Cocultivation of an ultrasmall environmental parasitic bacterium with lytic ability against bacteria associated with wastewater foams. Nat Microbiol 6:703–711.

8. Moreira D, Zivanovic Y, López-Archilla AI, Iniesto M, López-García P. 2021. Reductive evolution and unique predatory mode in the CPR bacterium Vampirococcus lugosii. Nat Commun 12:2454.

9. Yakimov MM, Merkel AY, Gaisin VA, Pilhofer M, Messina E, Hallsworth JE, Klyukina AA, Tikhonova EN, Gorlenko VM. 2022. Cultivation of a vampire: ‘ Candidatus Absconditicoccus praedator.’ Environ Microbiol 24:30–49.

10. Kuroda K, Yamamoto K, Nakai R, Hirakata Y, Kubota K, Nobu MK, Narihiro T. 2022. Symbiosis between Candidatus Patescibacteria and Archaea Discovered in Wastewater-Treating Bioreactors. MBio 13:e0171122.

11. Chen X, Molenda O, Brown CT, Toth CRA, Guo S, Luo F, Howe J, Nesbø CL, He C, Montabana EA, Cate JHD, Banfield JF, Edwards EA. 2023. “ Candidatus Nealsonbacteria” Are Likely Biomass Recycling Ectosymbionts of Methanogenic Archaea in a Stable Benzene-Degrading Enrichment Culture. Appl Environ Microbiol 89.

12. Kuroda K, Kubota K, Kagemasa S, Nakai R, Hirakata Y, Yamamoto K, Nobu MK, Narihiro T. 2022. Novel Cross-domain Symbiosis between *Candidatus* Patescibacteria and Hydrogenotrophic Methanogenic Archaea *Methanospirillum* Discovered in a Methanogenic Ecosystem. Microbes Environ 37:ME22063.

13. Touzel JP, Prensier G, Roustan JL, Thomas I, Dubourguier HC, Albagnac G. 1988. Description of a new strain of Methanothrix soehngenii and rejection of Methanothrix concilii as a synonym of Methanothrix soehngenii. Int J Syst Bacteriol 38:30–36.

14. Firtel M, Southam G, Harauz G, Beveridge TJ. 1993. Characterization of the cell wall of the sheathed methanogen Methanospirillum hungatei GP1 as an S layer. J Bacteriol 175:7550–7560.

15. Chaumeil P-A, Mussig AJ, Hugenholtz P, Parks DH. 2022. GTDB-Tk v2: memory friendly classification with the genome taxonomy database. Bioinformatics 38:5315–5316.

16. Xie B, Wang J, Nie Y, Tian J, Wang Z, Chen D, Hu B, Wu X-L, Du W. 2022. Type IV pili trigger episymbiotic association of Saccharibacteria with its bacterial host. Proc Natl Acad Sci 119:2017.

17. McLean JS, Bor B, Kerns KA, Liu Q, To TT, Solden L, Hendrickson EL, Wrighton K, Shi W, He X. 2020. Acquisition and Adaptation of Ultra-small Parasitic Reduced Genome Bacteria to Mammalian Hosts. Cell Rep 32:107939.

18. Castelle CJ, Brown CT, Anantharaman K, Probst AJ, Huang RH, Banfield JF. 2018. Biosynthetic capacity, metabolic variety and unusual biology in the CPR and DPANN radiations. Nat Rev Microbiol 16:629–645.

19. Seymour CO, Palmer M, Becraft ED, Stepanauskas R, Friel AD, Schulz F, Woyke T, Eloe-Fadrosh E, Lai D, Jiao J-Y, Hua Z-S, Liu L, Lian Z-H, Li W-J, Chuvochina M, Finley BK, Koch BJ, Schwartz E, Dijkstra P, Moser DP, Hungate BA, Hedlund BP. 2023. Hyperactive nanobacteria with host-dependent traits pervade Omnitrophota. Nat Microbiol 8:727–744.

20. Chatterjee S, Basak AJ, Nair A V., Duraivelan K, Samanta D. 2021. Immunoglobulin-fold containing bacterial adhesins: molecular and structural perspectives in host tissue colonization and infection. FEMS Microbiol Lett 368:1–14.

21. Nguyen VS, Spinelli S, Cascales É, Roussel A, Cambillau C, Leone P. 2021. Anchoring the T6SS to the cell wall: Crystal structure of the peptidoglycan binding domain of the TagL accessory protein. PLoS One 16:e0254232.

22. Capitani G, Rossmann R, Sargent DF, Grütter MG, Richmond TJ, Hennecke H. 2001. Structure of the soluble domain of a membrane-anchored thioredoxin-like protein from Bradyrhizobium japonicum reveals unusual properties. J Mol Biol 311:1037–1048.

23. Reid CW, Blackburn NT, Legaree BA, Auzanneau F-I, Clarke AJ. 2004. Inhibition of membrane-bound lytic transglycosylase B by NAG-thiazoline. FEBS Lett 574:73–79.

24. Jumper J, Evans R, Pritzel A, Green T, Figurnov M, Ronneberger O, Tunyasuvunakool K, Bates R, Žídek A, Potapenko A, Bridgland A, Meyer C, Kohl SAA, Ballard AJ, Cowie A, Romera-Paredes B, Nikolov S, Jain R, Adler J, Back T, Petersen S, Reiman D, Clancy E, Zielinski M, Steinegger M, Pacholska M, Berghammer T, Bodenstein S, Silver D, Vinyals O, Senior AW, Kavukcuoglu K, Kohli P, Hassabis D. 2021. Highly accurate protein structure prediction with AlphaFold. Nature 596:583–589.

Figure legends

Figure 1 (A) Cell length proportions of clear and weak fluorescence of *Methanothrix* filamentous cells calculated based on the fluorescence *in situ* hybridization signals using the *Methanothrix*-targeting MX825-FITC probe and *Candidatus* Yanofskybacteria-targeting Pac_683-Cy3 probe. The *Methanothrix* cells attached with > 5 *Ca*. Yanofskybacteria cells were chosen for calculation. (B) Proportions of detected *Ca*. Yanofskybacteria cells attached to the different fluorescence of *Methanothrix* cells: attached to *Methanothrix* filamentous cells with clear fluorescence, attached to *Methanothrix* with weak fluorescence, and attached to *Methanothrix* with no fluorescence. (C) The fluorescence of *Methanospirillum* cells with or without 32-520 cells. (D) FISH brightness of measured *Methanothrix* filamentous cells based on 8-bit grayscale images. (A)–(D) Different letters in the figure indicate significant differences among the values of the proportions based on Tukey's test ($p < 0.05$). (E)–(I) Transmission electron micrographs of small submicron cells attached to (E)–(H) *Methanothrix*-like cells and (I) and (J) *Methanospirillum*-like cells in culture system C-1 on Day 33. Orange arrows indicate extracellular substances at the attachment sites.

Figure 2 (A)–(D) Scanning electron micrographs of small submicron cells (yellow arrows) attached to (A) and (B) *Methanothrix*-like cells and (C) and (D) *Methanospirillum*-like cells in culture system C-1 on Day 33. White arrows indicate extracellular substances at the attachment sites. (E) Gene expression heatmap of the five most highly expressed genes with signal peptides in the genome of *Candidatus* Yanofskybacteria/UBA5738 (PMX.810_sub) and 32-520/UBA5633 (PMX.50 and PMX.108) in culture systems C-2–C-4 on Day 14 and C-6 and C-7 on Day 31. The color scale from white to orange shows the gene expression level based on the normalized RPKM value (see Text S1). "Days 31/14" indicates the difference in gene expression between Days 31 and 14. (F) Predicted protein structures of the

highly expressed genes of *Ca*. Patescibacteria using the AlphaFold2 software package (24). The overlaying domain was predicted through the InterPro database (http://www.ebi.ac.uk/interpro/). PGBD, Ig-like, and PKD are the peptidoglycan binding domain, immunoglobulin-like domain, and polycystic kidney disease domain, respectively.

Legends of Supplemental materials

Supporting Information The file containing materials and methods and results and discussion.

Figure S1 Phylogenetic trees of order *Candidatus* Paceibacterales based on (A) 16S rRNA gene sequences and (B) concatenated phylogenetic marker genes of GTDBtk 2.0.0 (ver. r207) (15). The phylogenetic positions of the metagenomic bins PMX_810 and PMX.108/PMX.50 are shown in pink and blue, respectively. The 16S rRNA gene-based tree was constructed using the neighbor-joining method. Sequences that match the Pac_683 and 32-520-1066 probes are shown in yellow and blue layers, respectively.

Figure S2 (A) Relative abundance of predominant *Candidatus* Patescibacteria and methanogenic archaea in the culture systems based on 16S rRNA gene sequencing. (B)–(D) Linear regression analysis between predominant methanogens and *Ca*. Patescibacteria based on 16S rRNA gene-based relative abundance. (B) *Methanothrix* OTU0004 and *Ca*. Yanofskybacteria OTU0011, (C) *Methanospirillum* OTU0025 and 32-520 OTU0014, and (D) *Methanospirillum* OTU0025 and 32-520 OTU0072.

Figure S3 (A) Number of *Candidatus* Yanofskybacteria cells attached to one *Methanothrix* filamentous cell on Days 14 and 31. (B) Number of 32-520 cells attached to one *Methanospirillum* cell on Days 14 and 31. The statistical analysis was performed based on Welch's t test.

Figure S4 Micrographs of (A) and (E) phase-contrast, (B) and (F) 4',6-diamidino-2-phenylindole dihydrochloride staining, (C), (D), (G), and (H) fluorescence *in situ* hybridization obtained from the culture system C-1 on (A)–(D) Days 14 and (G)–(H) 31. (C) and (G) *Ca*. Yanofskybacteria-targeting Pac_683-Cy3 probe and (D) and (H) *Methanothrix*-targeting MX825-FITC probe.

334 **Figure S5** Micrographs of (A) and (E) phase-contrast, (B) and (F) 4',6-diamidino-2-
335 phenylindole dihydrochloride (DAPI) staining, (C), (D), (G), and (H) fluorescence *in situ*
336 hybridization obtained from the culture system C-1 on (A)–(D) Days 14 and (G)–(H) 31. (C)
337 and (G) 32-520-targeting 32-520-1066-Cy3 probe and (D) and (H) Archaea-targeting
338 ARC915-FITC probe. Yellow arrows indicate FISH-detectable 32-520 cells. Light blue
339 arrows indicate unspecific FISH signals that were not observed by phase-contrast and DAPI
340 staining. Dashed white lines indicate weak or no FISH signals of *Methanospirillum*-like cells.
341
342 **Table S1** Mapped and total sequence reads of the metatranscriptome in this study.
343 **Table S2** Summary of the gene expression level and annotation of metagenomic bins of
344 *Candidatus* Yanofskybacteria/UBA5738 (PMX_810_sub) and 32-520/UBA5633 (PMX.50
345 and PMX.108) using DRAM, BlastKOALA, and SignalP annotation software.
346 **Table S3** Summary of the gene expression level and annotation of metagenomic bins of
347 *Methanothrix* (PMX.81, PMX.12, and PMX.35) and *Methanospirillum* (PMX.141_sub) using
348 DRAM, BlastKOALA, and SignalP annotation software.
349 **Table S4** Summary of the annotation of the secretion systems, transporter-related proteins,
350 ATPase, and cell growth-related genes in the genome of *Candidatus*
351 Yanofskybacteria/UBA5738 (PMX.810_sub) and 32-520/UBA5633 (PMX.50 and PMX.108)
352 in culture systems C-2–C-4 on Day 14 and C-6 and C-7 on Day 31.
353

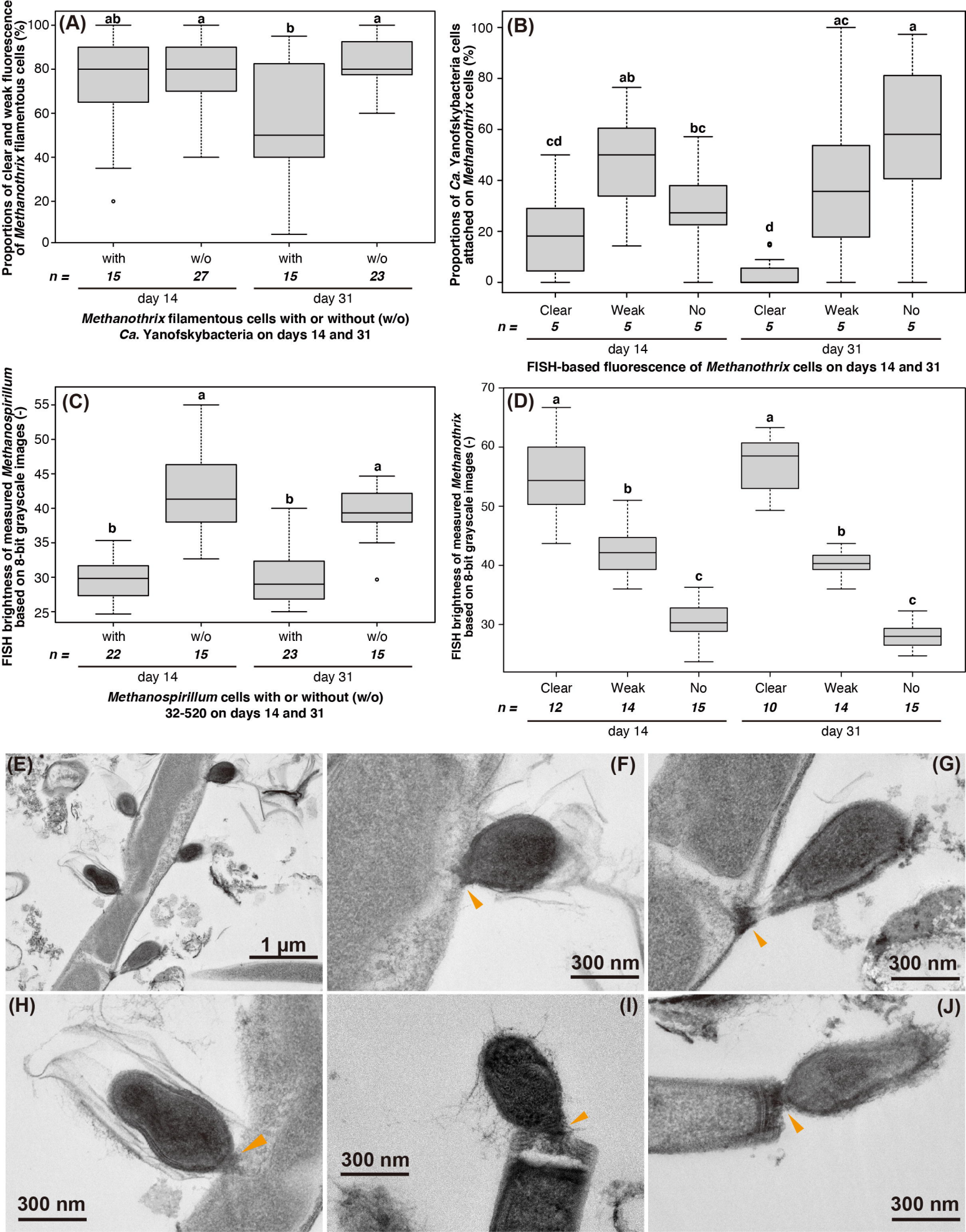
(A)
Proportions of clear and weak fluorescence of Methanothrix filamentous cells (%)
ab
a
b
a
with
w/o
with
w/o
n =
15
27
15
23
day 14
day 31
Methanothrix filamentous cells with or without (w/o) Ca. Yanofskybacteria on days 14 and 31
(B)
Proportions of Ca. Yanofskybacteria cells attached on Methanothrix cells (%)
cd
ab
bc
d
ac
a
Clear
Weak
No
Clear
Weak
No
n =
5
5
5
5
5
5
day 14
day 31
FISH-based fluorescence of Methanothrix cells on days 14 and 31
(C)
FISH brightness of measured Methanospirillum based on 8-bit grayscale images (-)
b
a
b
a
with
w/o
with
w/o
n =
22
15
23
15
day 14
day 31
Methanospirillum cells with or without (w/o) 32-520 on days 14 and 31
(D)
FISH brightness of measured Methanothrix based on 8-bit grayscale images (-)
a
b
c
a
b
c
Clear
Weak
No
Clear
Weak
No
n =
12
14
15
10
14
15
day 14
day 31
(E)
1 µm
(F)
300 nm
(G)
300 nm
(H)
300 nm
(I)
300 nm
(J)
300 nm

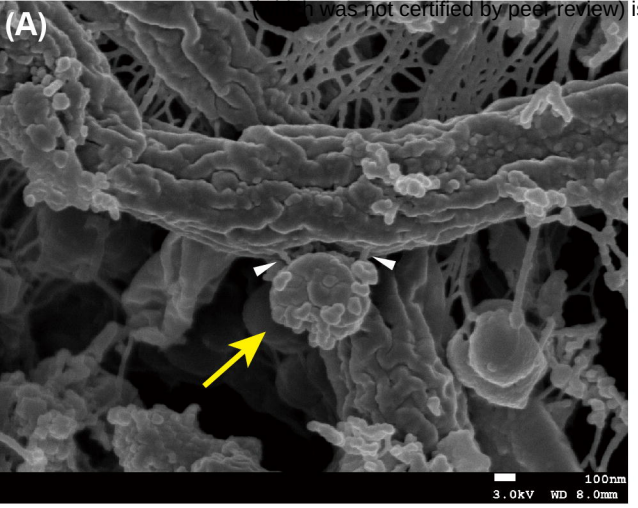

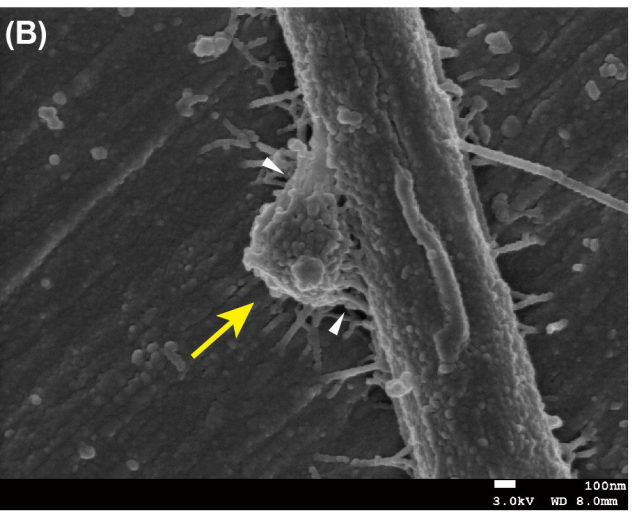

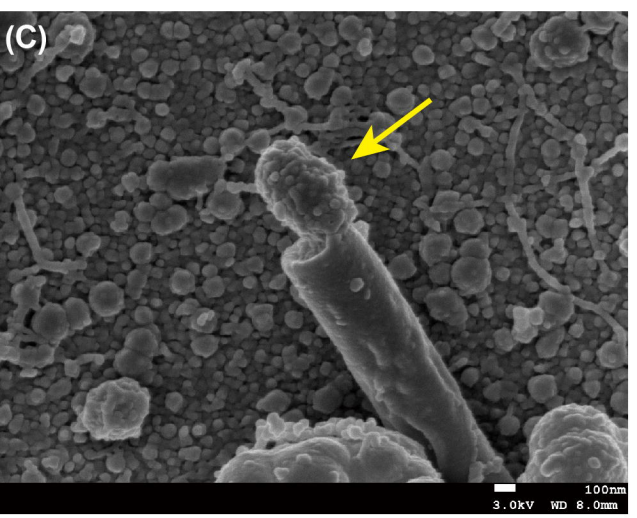

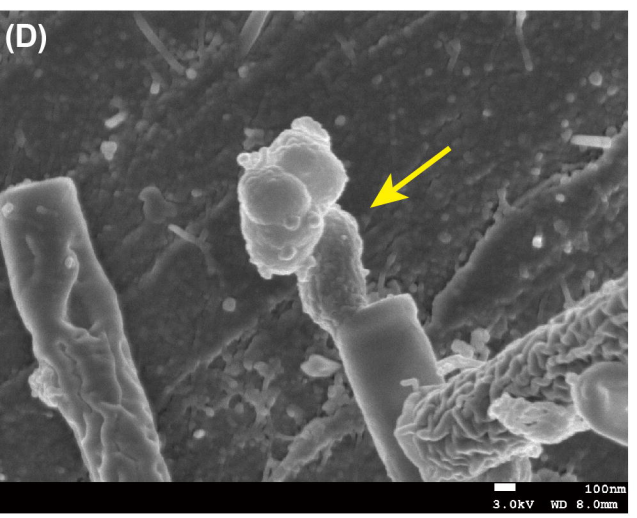

(E)

Locus	length (bp)	Gene expression level [log_2(RPKM+1)] day 14	day 31	days 31/14
PMX_810_sub_00350	2079	16.7	15.9	-0.8
PMX_810_sub_00356	1116	15.9	15.2	-0.7
PMX_810_sub_00650	591	15.0	15.0	-0.1
PMX_810_sub_00504	441	13.6	13.4	-0.2
PMX_810_sub_00811	408	13.4	16.3	2.9
PMX_810_sub_00465	1320	12.9	13.9	1.0
PMX.108_01129	1083	11.5	12.2	0.6
PMX.108_01191	1107	10.2	8.1	-2.2
PMX.108_00341 (pilin)	300	9.9	0.0	-9.9
PMX.108_00302	3558	9.8	7.9	-1.8
PMX.108_00880	309	9.1	7.9	-1.3
PMX.108_00119	399	8.3	8.8	0.5
PMX.108_00787	1278	0.0	8.1	8.1
PMX.50_00411	3891	12.0	14.1	2.1
PMX.50_00003	1254	11.3	13.6	2.4
PMX.50_00607 (pilin)	429	10.2	12.1	1.9
PMX.50_00002	1362	10.2	13.7	3.5
PMX.50_00571 (pilin)	396	9.6	8.7	-0.9
PMX.50_00608 (pilin)	339	9.4	11.8	2.4

(F)